CHAPTER 9
Artifacts

Artifacts in MR images refer to pixels that do not faithfully represent the anatomy being studied. In the images, the general appearance is that the underlying anatomy is visualized but spurious signals are present that do not correspond to actual tissue at that location. The artifacts may or may not be easily discernible from normal anatomy, particularly if they are of low intensity, and may or may not be reproducible. Artifacts can be categorized in many ways. One approach divides them into three groups, according to the cause of the signal misregistration. The first group is a consequence of motion of patient tissue during the measurement. This includes both gross physical motion by the patient and internal physiological motion such as blood flow. The second group is produced primarily as a result of the particular measurement technique and/or specific measurement parameters. The final group of artifacts are independent of the patient or measurement technique, being generated either through a malfunction of the MR scanner during data collection or from a source external to the patient or scanner.

9.1 Motion artifacts

Motion artifacts occur as a result of movement of tissue during the data acquisition period. They are manifest as signal misregistrations in the phase encoding direction, though the specific appearance of the artifact depends on the nature of the motion and the particular measurement technique. The artifacts are caused by tissue that is excited at one location, producing signals that are mapped to a different location during detection. As mentioned in Chapter 4, the typical MRI scan excites and detects a signal from a tissue volume multiple times with the phase encoding gradient G_{PE} changing amplitude prior to signal detection. The assumption is made that any measured signal intensity variations from one measurement to the next are as a result of G_{PE} only. When tissue moves, the protons are at a different location at the time of detection and experience a different G_{RO} amplitude, contributing a different frequency and phase for that measurement. The Fourier transformation mismaps these protons to an incorrect location along the phase encoding direction in the image. The misregistered signals occur along the phase encoding direction rather than the readout direction because G_{RO} is identical for each signal that is measured, while G_{PE} changes from line to line. In addition, the encoding

MRI Basic Principles and Applications, Fifth Edition.
Brian M. Dale, Mark A. Brown and Richard C. Semelka.
© 2015 John Wiley & Sons, Ltd. Published 2015 by John Wiley & Sons, Ltd.

of phase by G_{PE} occurs prior to signal detection while it occurs concurrent with signal detection for G_{RO}. In general, many measurements are made in the production of an image, each with a different amount of motion contamination.

The sensitivity of a measurement to tissue motion depends on the amount of frequency and phase variation that occurs between successive echoes due to the tissue movement. If the motion occurs during measurements with high positive or negative G_{PE} (at the edges of *k*-space), then the misregistered signal will have very little amplitude and will generate minimal artifact regardless of the nature of the motion. If the motion occurs during measurements with low amplitude G_{PE} (low magnitude k_y), the nature of the motion and the measurement technique will affect the artifact appearance. If the echo timing is relatively slow or the motion is at a moderate rate, significant artifact will be generated since there will be significant signal measured from different locations. If the time between successive echoes (echo spacing in echo train sequences, *TR* for traditional sequences) is rapid and the motion is relatively slow, the echoes near the center of *k*-space may be acquired with the tissue in the same location, so that there is minimal artifactual signal generated. This is the principle behind the use of single-shot ETSE for visualizing the small bowel.

The artifact appearance also depends on the nature of the motion. If the motion itself is periodic, then the misregistration artifacts will be discrete in nature, often referred to as "ghosts". The "ghost" signals will offset in the phase encoding direction from the primary anatomy at locations inversely proportional to the difference between the period of the motion and the *TR* of the scan. The sequence looping may also affect which images of the scan will show motion artifacts, subject to the G_{PE} discussion above. For scans with one subloop, all images will generally exhibit motion artifacts. For scans with multiple subloops, artifacts will be present for all images within a subloop where the motion occurs. When interleaved acquisition ordering is used, images at adjacent slice positions may show different amounts of artifact contamination.

Probably the most common motion artifact in MRI is due to blood flow. The artifact from blood flow is dependent on the nature of the flow and its direction relative to the slice orientation. Through-plane flow (flow that is perpendicular to the slice plane) typically produces a localized artifact in the image with a width equal to the vessel diameter and in line with the source of the flow. Flow that is relatively fast compared to *TR* will produce a relatively continuous artifact throughout the FOV, such as in spin echo images (Figure 9.1a). Flow that is slow relative to *TR* may not generate an artifact as significant saturation will occur unless a contrast agent is used to shorten the *T1* relaxation time of the blood. If the flow is relatively periodic such as pulsatile flow, then the artifact appears as "ghost" vessels at discrete intervals. This is often seen from blood flow in the aorta or inferior vena cava (IVC) in transverse slices of the abdomen acquired with gradient echo images (Figure 9.1b). In-plane flow (flow that is parallel to the slice plane) produces a more diffuse artifact, which can be observed from the aorta and IVC in coronal images. The vessel extends through the entire image field and thus the artifact affects all regions of the image (Figure 9.2a). Flow of the cerebrospinal fluid in the brain and spinal canal are also problematic and can produce analogous artifacts on *T2*-weighted images (Figure 9.2b).

In abdominal or lumbar spine imaging, respiratory motion and peristalsis are the most common causes of a severe artifactual signal. The movement of the abdomen during the data collection process produces multiple misregistration artifacts. If the respiration rate is constant, the "ghost" images are either few in number or discrete and offset in the phase encoding direction from the true image by an amount proportional to the respiration rate.

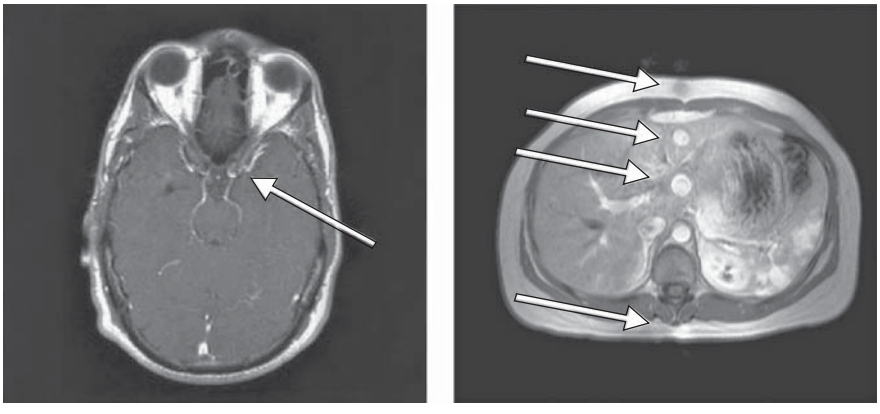

(a) (b)

Figure 9.1 Flow misregistration artifact, through-plane. (a) Flow fast compared to measurement technique produces "zipper"-like artifact (arrow). Measurement technique: pulse sequence, spin echo; *TR*, 479 ms; *TE*, 17 ms; acquisition matrix, N_{PE}, 192 and N_{RO} 256; FOV, 172 mm PE × 230 mm RO; N_{SA}, 1; slice thickness, 5 mm. PE direction: R–L; RO direction: A–P. (b) Periodic flow from the aorta will be misregistered as multiple ghosts (arrows). Measurement parameters are: pulse sequence, two-dimensional spoiled gradient echo; *TR*, 164 ms; *TE*, 4 ms; excitation angle, 70°; acquisition matrix, N_{PE}, 134 and N_{RO} 256; FOV, 262 mm PE × 350 mm RO; N_{SA}, 1; slice thickness, 5 mm; PE direction, A–P; RO direction, L–R.

If the respiration rate is variable, the "ghost" images are numerous and appear as a smearing of signal throughout the entire image (Figure 9.3a). For segmented techniques such as echo train spin echo techniques, respiratory motion may appear as multiple lines or so-called "venetian blinds" superimposed throughout the entire FOV in the phase encoding direction. The number and spacing of the lines is based on the number of segments for the scan (Figure 9.3b). Peristalsis produces motion artifacts that are less distinct than those from respiratory motion. In most instances, a general blurring of the large and small bowel occurs and a layer of noise is superimposed over the entire image.

9.2 Sequence/Protocol-related artifacts

A second class of artifacts results from the specific measurement process used to acquire the image. While the appearance of motion artifacts also depends on the particular measurement protocol, this group of artifacts is more sensitive to technical aspects of the particular pulse sequence and method of data collection used. The source of these artifacts is relatively constant over the course of the measurement and the resulting signal misregistrations are easily recognized when present.

9.2.1 Aliasing

The techniques used for spatial localization assign a unique frequency and phase to each location within the image. These are determined by the acquisition matrix and the desired FOV

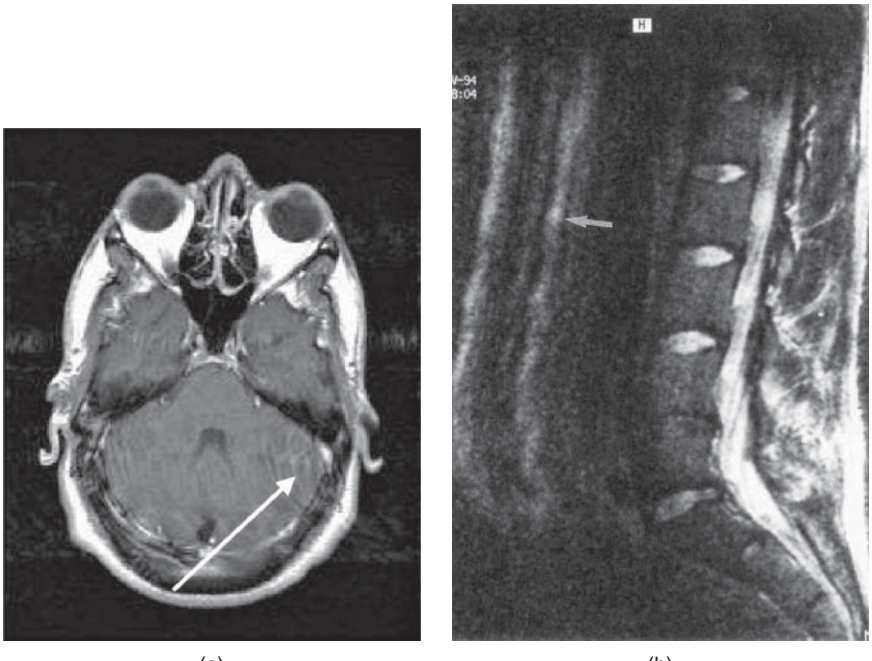

(a) (b)

Figure 9.2 Flow misregistration artifact, in-plane. (a) In-plane blood flow will produce severe signal misregistration (arrow). Measurement technique: pulse sequence, spin echo; *TR*, 479 ms; *TE*, 17 ms; acquisition matrix, N_{PE}, 192 and N_{RO}, 256; FOV, 172 mm PE × 230 mm RO; N_{SA}, 1; slice thickness, 5 mm; PE direction: R–L; RO direction: A–P. (b) Flow misregistration artifact. Flowing CSF will be misregistered as a ghost canal (arrow). Measurement parameters are: pulse sequence, spin echo; *TR*, 2500 ms; *TE*, 90 ms; excitation angle, 90°; acquisition matrix, N_{PE}, 192 and N_{RO}, 256 with twofold frequency oversampling; FOV, 210 mm PE × 280 mm RO; N_{SA}, 1; slice thickness, 5 mm; PE direction, A–P; RO direction, H–R.

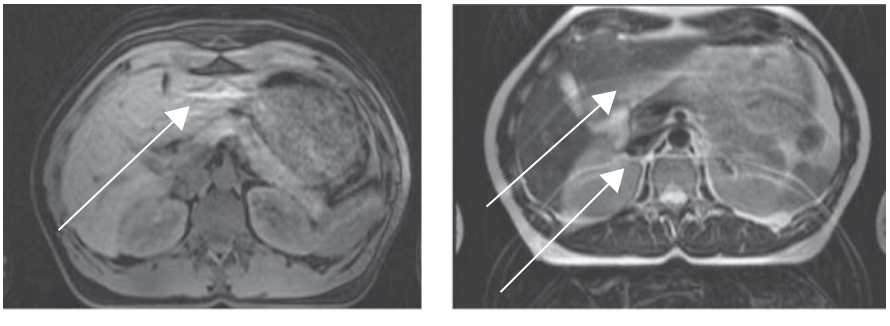

(a) (b)

Figure 9.3 Respiratory motion artifact. Extraneous ghost images are generated due to motion of the abdominal wall during data acquisition (arrows). The number and severity of the ghosts depends on the *TR*, respiration rate, and the particular measurement technique. (a) Pulse sequence, two-dimensional spoiled gradient echo; *TR*, 159 ms; (b) pulse sequence, echo train spin echo; *TR*, 4000 ms.

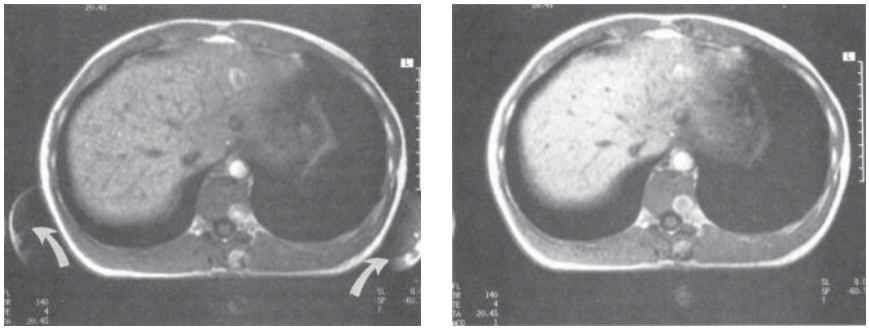

(a) (b)

Figure 9.4 Effects of oversampling. (a) Without frequency oversampling, frequencies for the protons within the arms exceed the Nyquist limit and are aliased or incorrectly mapped into the image (arrows). Measurement parameters are: pulse sequence, two-dimensional spoiled gradient echo; *TR*, 140 ms; *TE*, 4 ms; excitation angle, 80°; acquisition matrix, N_{PE}, 128 and N_{RO}, 256; FOV, 263 mm PE × 350 mm RO; N_{SA}, 1; slice thickness, 8 mm. (b) Same as (a) except with frequency oversampling. The frequencies for the protons within the arms are measured accurately by increasing the number of readout data points measured during the same sampling time while maintaining the same G_{RO}. Only frequencies corresponding to the FOV selected are stored so that the arms are excluded from the final image. Measurement parameters are the same as (a), except that $N_{RO} = 512$.

in the phase-encoding and readout directions. Aliasing in the readout direction occurs when tissue outside the chosen FOV_{RO} is excited. This can occur if an FOV_{RO} smaller than the anatomical slice is selected. The frequencies for this tissue exceed the Nyquist limit for the sampling conditions and are mapped to a lower frequency, a situation known as high-frequency aliasing or frequency wraparound (Figure 9.4a). The technique used to overcome this is known as frequency oversampling, in which the dwell time per point is reduced by increasing the number of readout data points while maintaining the same sampling time. The same G_{RO} is used, which results in an increase in the span of k_x using the same Δk. The oversampled data results in an increase of the Nyquist frequency ω_{NQ} for the measurement, according to equation (2.2). Because G_{RO} is constant, the frequencies at the chosen FOV_{RO} are unchanged, so that extraction of the central range of frequencies produces an image of the desired size and number of data points. For example, for a 256 × 256 matrix with twofold frequency oversampling, 512 data points are measured but only the central 256 data points are used to create the image (Figure 9.4b).

Aliasing can also occur in the phase encoding direction when tissue outside the FOV_{PE} are excited. The protons within this region undergo phase changes corresponding to frequencies greater than can be accurately measured for the G_{PE} pulse duration (Nyquist limit). They are mapped via the Fourier transformation to a lower phase, in a manner analogous to the aliasing in the readout direction described above. Phase encoding aliasing can only be eliminated by increasing the effective FOV_{PE} for the scan. This may be accomplished either by reducing the change in gradient amplitude Δk_y from one phase encoding step to the next (increasing the FOV_{PE}) or by increasing the number of phase changes (i.e., Nyquist frequency) while maintaining the same Δk_y, a technique known as phase encoding oversampling. Because more echoes are acquired, phase encoding oversampling will increase the total measurement time while also improving the SNR.

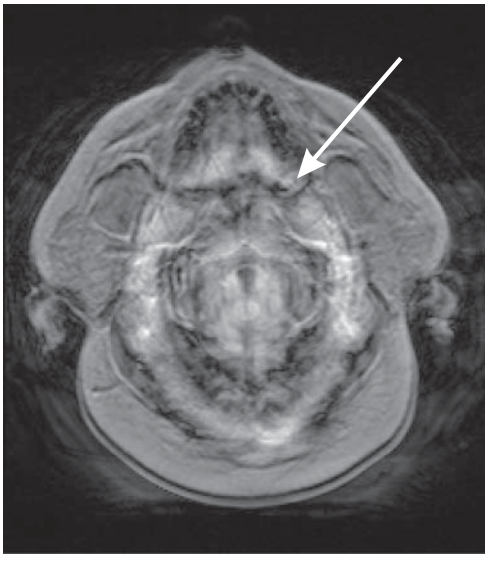

Figure 9.5 Three-dimensional volume scan showing high-frequency aliasing in the slice-selection direction. The superior part of the brain (arrow) appears in the inferior slices of the imaging volume.

Aliasing can also occur in the slice-selection direction in 3D scanning in certain situations. The excitation pulse must be nonselective and the k_z volume spanned by the 3D encoding table must be smaller than the volume of tissue excited. In this case, anatomy from slices at one edge of the volume will wrap into the opposite side of the volume (Figure 9.5). Similar to the case of aliasing in the phase-encoding direction, the remedy for aliasing in the slice direction is to increase the effective area of accurate measurement, either though increased Δk_z (increasing the effective slice thickness) or through slice oversampling (more k_z samples with constant Δk_z).

Parallel acquisition techniques can also show aliasing artifacts. As mentioned in Chapter 5, the measurement process uses larger Δk_y values compared to a conventional scan. As a result, the effective FOV_{PE} for a coil is smaller, so that aliasing occurs for the signal in each coil. If the image-based techniques are used, this aliasing is indistinguishable from aliasing produced if the base FOV_{PE} is too small for the anatomy under observation. This causes more severe aliasing artifacts than for the conventional scan (Figure 9.6a). Phase oversampling could be incorporated in the scan protocol, but this would increase the scan time. Increasing the base FOV_{PE} is the best option to eliminate the additional artifact. In contrast, the *k*-space-based techniques will generate more diffuse artifacts, with no additional aliasing artifacts (Figure 9.6b).

9.2.2 Chemical shift artifacts

Chemical shift-based artifacts arise from the inherent 3.5 ppm frequency difference between fat and water protons under the influence of an external magnetic field as described in Chapter 2. Two constant artifacts may be generated by this frequency difference. One is known as the chemical shift artifact, which is a misregistration of fat and water protons from a voxel that are mapped to different pixels. As described in Chapter 4, the detected signal from a voxel

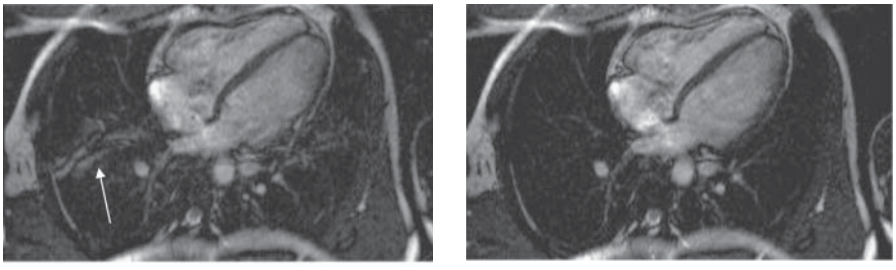

(a) (b)

Figure 9.6 Small FOV aliasing artifacts with parallel acquisitions: (a) image-based parallel acquisition; (b) *k*-space-based acquisition. Note the aliasing artifact in the lung field in (a) (arrow) due to the anatomical region being larger than the scan FOV. This area is artifact-free in (b).

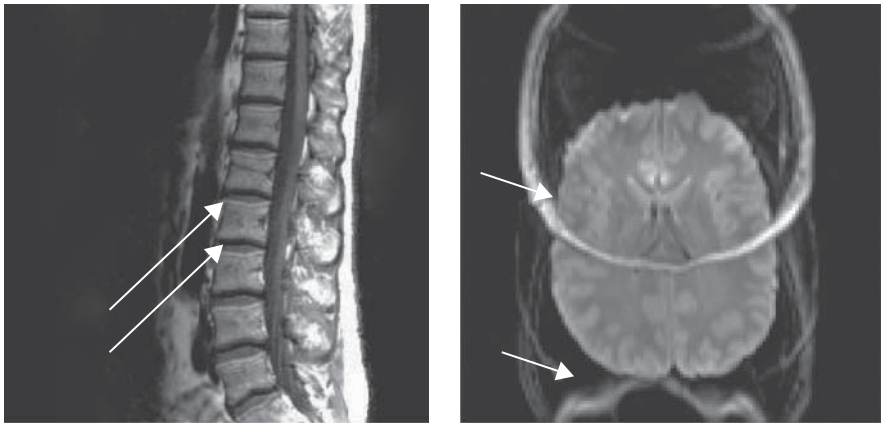

(a) (b)

Figure 9.7 Chemical shift artifact. (a) Note alternate bands of light and dark at the interface between the vertebrae and disk (arrows). Measurement parameters: pulse sequence, spin echo; Receiver bandwidth, 20 kHz; readout direction, H–F. (b) A complete misregistration of fat from the bone marrow of the skull (arrow). Measurement parameters are: pulse sequence, spin echo EPI; phase-encoding direction, A–P.

is mapped to a position based on its frequency according to equation (4.1), under the assumption that all protons within a voxel resonate at the same frequency. Due to the difference in molecular structure, fat protons have an intrinsically lower resonant frequency than water protons when exposed to the same external magnetic field. Fat protons within a voxel are affected by the same G_{RO} as the water protons but will be mapped to a lower frequency pixel in the readout direction. This frequency misregistration is not noticeable in tissues with a uniform fat–water content, but can be seen at the borders between tissues with a significantly different fat–water content; for example, between a disk and vertebrae in the spine or between the kidney and retroperitoneal fat. Parallel areas of bright and dark pixels can be visualized where the fat and water signals superimpose and where they do not, respectively (Figure 9.7a). The number of pixels corresponding to the chemical shift artifact (CSA) depends

upon the frequency difference in Hz between fat and water, the total receiver bandwidth, and the number of readout data points spanning the FOV_{RO}:

$$\text{CSA} = \Delta\omega * N_{RO}/BW_{REC} \tag{9.1}$$

At 1.5 T, the frequency difference, $\Delta\omega$, is approximately 220 Hz so that, for a scan with a total receiver bandwidth of 20 kHz and $N_{RO} = 256$, the CSA will be 2.8 pixels. The severity of the artifact in the final image will depend on the FOV_{RO}. If an FOV_{RO} of 350 mm is used, this translates into a fat/water misregistration of 3.6 mm. For an FOV_{RO} of 175 mm, the artifact is only 1.8 mm. For a scan with a receiver bandwidth of 33 kHz, the CSA will be 1.7 pixels and a misregistration of 2.2 mm. Chemical shift artifacts are most prominent at magnetic field strengths greater than 1.5 T, using low or narrow receiver bandwidths and large FOV_{RO}, and at fat–water tissue interfaces. For example, at 3 T, the same 33 kHz receiver bandwidth and 256 readout points will produce a CSA of 3.4 pixels.

In theory, chemical shift artifacts are possible in all three directions (slice selection, phase encoding, and readout), since magnetic field variations (gradient pulses) are used for localization in all cases. In the slice selection direction, the RF pulse bandwidth and gradient amplitude are chosen to keep this at a minimum. In addition, because the slice selection direction is not directly visualized, any signal misregistration in this direction is difficult to discern. This may not be the case in MR spectroscopic scans, where there may be observable variations in signal amplitude at different locations within the slice (see Chapter 13).

The appearance of the chemical shift artifact in the readout and phase encoding directions depends on the particular pulse sequence. For routine imaging techniques such as spin echo, echo train spin echo, or gradient echo, the phase-encoding process is reinitiated following each excitation pulse. Since Δk_y is constant, fat and water protons located at the same position in the phase encoding direction undergo equal amounts of phase change. They are mapped to the same location in the image in the phase encoding direction and no artifact results. For these techniques, chemical shift artifacts may be observed in the readout direction, based on the specific criteria described previously. For echo planar imaging, the receiver bandwidth is normally very large (in excess of 100 kHz) so that fat and water frequencies are mapped to the same pixel. However, the phase encoding process for the entire image occurs in a continuous fashion following one or two excitation pulses. Chemical shift artifacts are observed in the phase-encoding direction and are very significant. Because the G_{PE} amplitude is very low, the misregistration may be as much as 12–15 pixels (Figure 9.7b). Use of fat suppression techniques is necessary to minimize the artifact.

9.2.3 Phase cancellation artifact

The second artifact induced by the chemical shift difference is known as the phase cancellation artifact (or sometimes the chemical shift artifact of the second kind), observed in out-of-phase gradient echo images. As shown in Figure 2.6, the fat protons cycle in phase relative to the water proton precession at a rate linearly proportional to the measurement time after the initial RF excitation pulse. For normal spin echo and fast spin echo sequences, this phase cycling is exactly reversed by the 180° RF pulse(s) so that the fat and water protons always contribute to the signal at the echo time, *TE*, with the same polarity; that is, the fat and water protons are described as "in phase" when the signal is detected regardless of the choice of *TE*. This assumes that the 180° RF pulse occurs halfway between the initial RF excitation pulse and *TE*. In gradient echo sequences, the phase cycling is not reversed (since there is no 180° RF pulse)

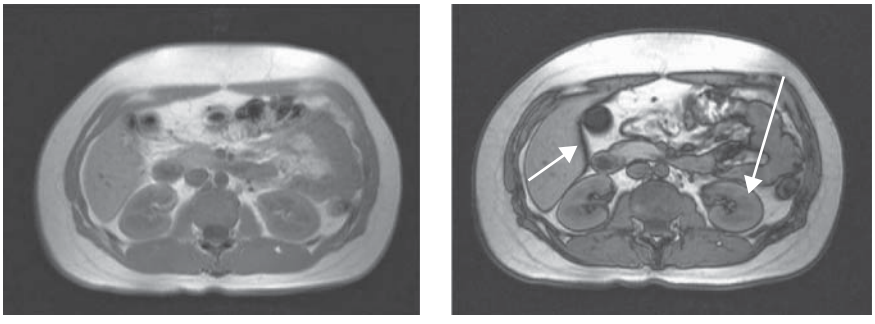

(a) (b)

Figure 9.8 Phase cancellation artifact. Other measurement parameters are: pulse sequence, two-dimensional spoiled gradient echo; *TR*, 164 ms; excitation angle, 70°; acquisition matrix, N_{PE}, 134 and N_{RO}, 256; FOV, 263 mm PE × 350 mm RO; N_{SA}, 1; slice thickness, 9 mm. (a) In-phase image (*TE*, 4.5 ms). Fat and water protons have the same phase and contribute in the same fashion to the image contrast. (b) Out-of-phase image (*TE*, 2.2 ms). Fat and water protons have opposite phases and contribute in opposite fashion to the image contrast. For voxels with equal amounts of fat and water, such as at the interface between liver or kidney and retroperitoneal fat, cancellation of signal occurs, producing a dark band (arrows).

so that fat and water protons contribute differently to the detected signal, depending on the particular *TE*. Voxels containing both fat and water have additional signal intensity variations in addition to those due to relaxation. For certain choices of *TE*, known as "out-of-phase" *TE*, very little signal is produced if the voxel has equal water and fat content, such as those voxels located at interfaces between fat- and water-based tissues. This signal cancellation appears as a dark ring surrounding the tissue (Figure 9.8).

The *TE* values that generate this phase cancellation depend on the magnetic field strength, since the time for the phase cycling depends upon the resonant frequency difference, $\Delta\omega$ in Hz, between fat and water:

$$TE_{\text{in-phase}} = n/\Delta\omega \tag{9.2}$$

where n is an integer. The out-of-phase *TE* times occur midway between the in-phase times (Table 9.1). Out-of-phase images are often used to assess the amount of fat contribution to a voxel. The phase cancellation artifact observed using out-of-phase *TE* makes it difficult to assess the interface of tissues with different fat and water content. The phase cycling also affects the signal content of all tissues throughout the image.

Table 9.1 Phase cycling *TE* times.

Field strength, T	In-phase *TE*, ms	Out-of-phase *TE*, ms
0.5	13.3, 26.67	6.67, 20
1.0	6.67, 13.3, 20	3.3, 10, 16.67
1.5	4.5, 9.0, 13.5, 18.0	2.25, 6.75, 11.25, 15.75
3.0	2.25, 4.5, 6.75, 9.0	1.12, 3.38, 5.63, 7.88

9.2.4 Truncation artifacts

Truncation artifacts are produced by insufficient digital sampling of the echo. The most common instance of this condition occurs when data collection is terminated while significant signal is still being induced in the receiver coil by the protons; for example, in *T1*-weighted imaging where there is a high signal from fat still present at the end of data collection. The Fourier transformation of this truncated data set produces a "ringing" type of signal oscillation that emanates from the edge of the anatomy (Figure 9.9). Truncation artifacts can also occur if the echo is sampled in an asymmetrical fashion; that is, the echo is not sampled equally on both sides of the echo maximum (Figure 9.10). This type of data sampling is often used in very short *TE* sequences (<3 ms) to minimize the receiver bandwidth.

Reduction of truncation artifacts involves reducing the signal amplitude so that it is minimal at the beginning or end of the data collection period. This reduction can be achieved in two ways. One approach is to reduce the fat signal through fat suppression (since fat typically has the largest signal in *T1*-weighted images), either using a fat saturation pulse or using an inversion recovery technique with an appropriate *TI* time. This approach changes the intrinsic image contrast and may be unacceptable for the particular clinical application. The other method is to apply an apodization filter to the raw data prior to Fourier transformation. This numerical process forces the signal amplitude to zero at the end of the data collection period. Several types of apodization filters have been developed (e.g., Fermi, Gaussian, Hanning), each with different characteristics regarding the filter shape (Figure 9.11). Use of apodization filters improves the signal-to-noise ratio by removing high-frequency noise from the signal. However, excessive filtering eliminates high frequencies responsible for fine spatial resolution or edge definition so that blurring is possible. Asymmetric echo sampling may require more extensive filtering to reduce truncation artifacts. Acquiring the echo in a symmetric fashion reduces the amount of filtering necessary.

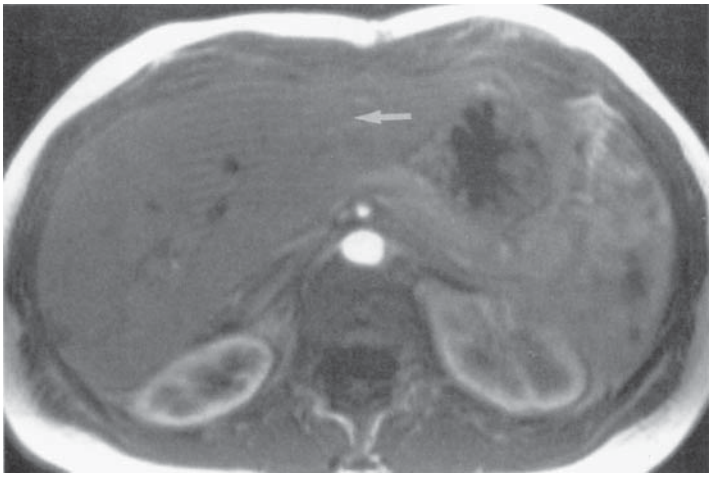

Figure 9.9 Truncation artifact. Image acquisition with asymmetric sampling produces a banding artifact (arrow), originating from the high signal of subcutaneous fat. Measurement parameters: pulse sequence, two-dimensional spoiled gradient echo; *TR*, 170 ms; *TE*, 4 ms; excitation angle, 80°; acquisition matrix, N_{PE}, 144 and N_{RO}, 256 with twofold oversampling; FOV, 262 mm PE × 350 mm RO; N_{SA}, 1.

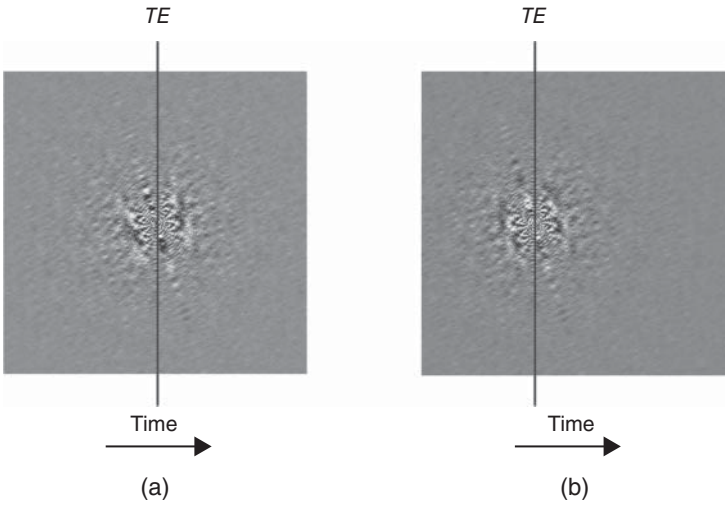

Figure 9.10 Symmetric versus asymmetric echo sampling. (a) In symmetric sampling, the echo is maximum (*TE*) midway through the sampling period, so that both sides of the echo signal are measured equally. Filtering of the data can be performed in a symmetrical fashion. (b) In asymmetric sampling, the echo maximum is in the early portion of the sampling period. Significant signal is present when the sampling begins and filtering of the signal is difficult.

9.2.5 Coherence artifacts

Coherence artifacts are a class of artifacts that can have a variable appearance, based on the particular measurement technique and how it is implemented on the scanner. They are produced by the RF pulses generating unwanted transverse magnetization that contributes to the detected signal. One coherence artifact is known as an FID artifact. As mentioned in Chapter 4, the RF excitation pulses are not uniform in profile. For instance, while most of the protons in a slice would experience a 180° excitation pulse, those located at the edges of the slice would experience a range of excitation angles, all less than 180°. The FID produced by these protons may still have significant amplitude when the desired echo signal is measured. Because the 180° RF pulse normally occurs after the phase encoding gradient during sequence execution, the induced signal will contribute identically during each ADC sampling period. The resulting artifact is a line of constant phase in the final image that is superimposed on the line of zero phase (Figure 9.12).

Another coherence artifact may be produced by the effects of the multiple RF excitation pulses on the protons. The spin echoes used to produce *T1*- and *T2*-weighted images are but two of several echoes generated by RF excitation pulses within an imaging sequence. For example, a series of three RF pulses such as a presaturation pulse and a 90–180° pulse pair or a 90–180–180° pulse trio may generate four or five echoes. The timing and number of echoes depends on the exact spacing of the pulses (Figure 9.13). The amplitude of each echo depends on the excitation angle of the individual pulses and the particular tissues being measured. These "secondary" echoes contain all the frequency information of the so-called primary echoes normally used, but have different *T1* and *T2* weighting to the signals. Should these other echoes occur while the ADC is sampling the primary echoes, they will contribute to the final image. These "extra" echoes may produce either line artifacts if not phase encoded or an

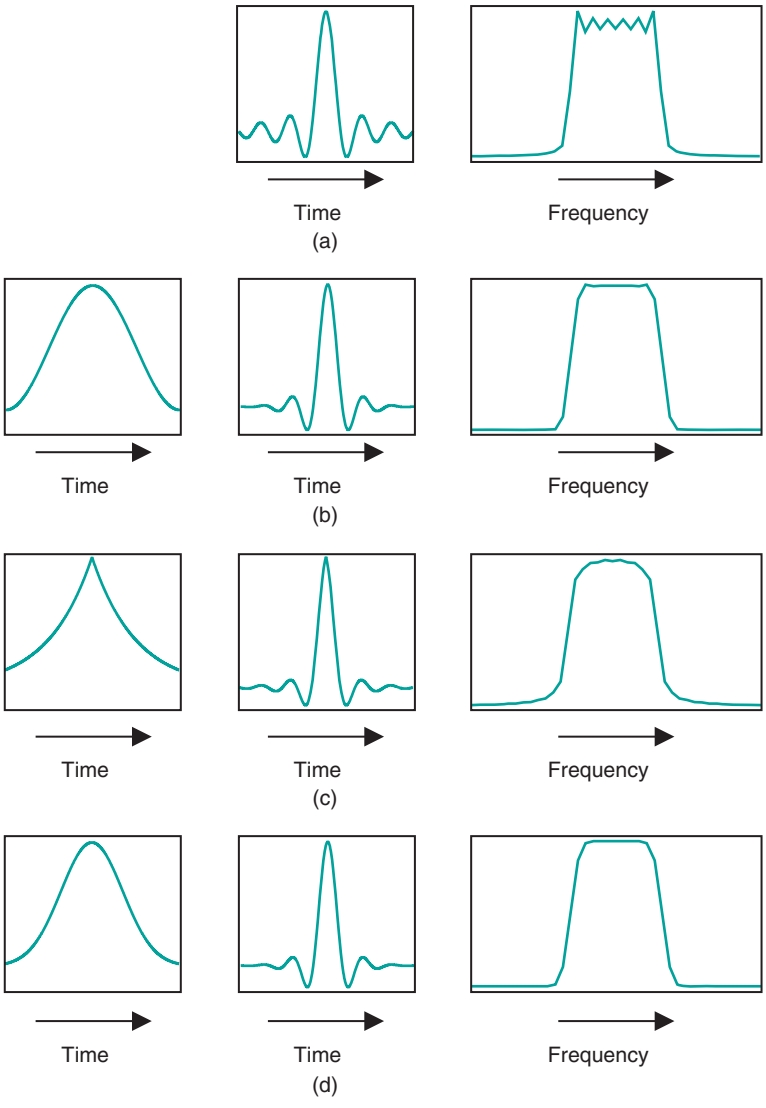

Figure 9.11 Raw data filtering. All vertical and horizontal scales are maintained in all figures. (a) Unfiltered sinc pulse waveform, time domain (left) and magnitude frequency domain (right) (note sawtooth pattern at top of right figure); (b) Gaussian filter (left), Gaussian-filtered sinc pulse waveform, time domain (center) and magnitude frequency domain (right). (note that sawtooth pattern at top of right figure is reduced but still present); (c) Fermi filter (left), Fermi-filtered sinc pulse waveform, time domain (center) and magnitude frequency domain (right) (note rounded top and large width at base of right figure); (d) Hanning filter (left), Hanning-filtered sinc pulse waveform, time domain (center) and magnitude frequency domain (right).

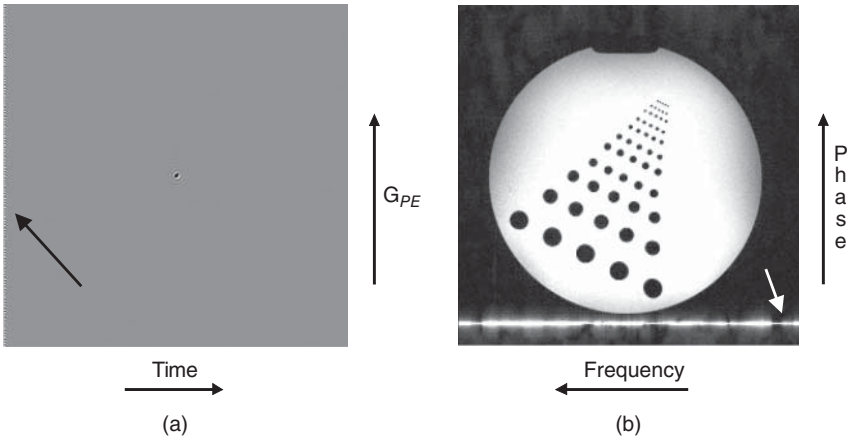

Figure 9.12 Insufficient spoiling, raw data and image. Due to the imperfect nature of RF pulses, additional signal can be produced by spins at the edge of the slice. If the spurious signal is generated by the 180° pulse in a spin echo pulse sequence, it is not affected by the phase encoding process and appears as a constant signal in *k*-space (arrow in a). The resulting image shows a bright line near the edge of the image FOV (arrow in b).

additional image if phase encoded (Figure 9.14). One of these echoes, known as the stimulated echo, is incorporated into the design of fast spin echo imaging techniques and in the volume selection process used in MR spectroscopy (Chapter 13).

Pulse sequences are usually designed with great care to minimize the contamination of the desired echo signals by the undesired echoes. When these undesired echoes form during the ADC sampling period due to the particular RF pulse timing, some form of coherence "spoiling" is used. Two approaches are used to minimize the coherence present from these secondary echoes during sampling. The most common method is to include additional gradient pulses applied at appropriate times during the pulse sequence, an approach known as gradient spoiling. The goal is to change the time when the coherence forms so that it occurs when the ADC is not sampling. These gradient pulses are usually of high amplitude and/or long duration. The time when these pulses are applied depends on which coherence is to be spoiled and what *TE* is chosen. Spoiler gradients applied following the 180° refocusing pulse reduce the FID artifact resulting from nonuniform RF excitation. Spoiler gradients following the data collection such as those used in spin echo sequences (see Figure 6.2) minimizes coherence contamination of the subsequent echoes. Gradient spoiling may also use a series of amplitudes rather than a constant amplitude pulse in order to improve spoiling if the RF interpulse time is short.

If the *TR* is short compared to the tissue *T2*, as is frequently used in gradient echo scanning, then significant coherence artifacts can occur from the standard RF excitation pulses. Use of gradient spoiling requires gradient pulse durations that can be 30–50% of the slice loop. For spoiled gradient echo sequences, another approach for spoiling is frequently used, known as RF spoiling. Normal data acquisition techniques apply RF pulses of constant phase or with a 180° phase alternation of the excitation pulse (i.e., +90°, –90°, +90°, …). The receiver is also phase-alternated to match the transmitter phase so that signal averaging can be performed. RF spoiling applies a phase variation other than ±90° or ±180° to the excitation pulse and receiver. The desired echo signals add in a coherent fashion, while the other

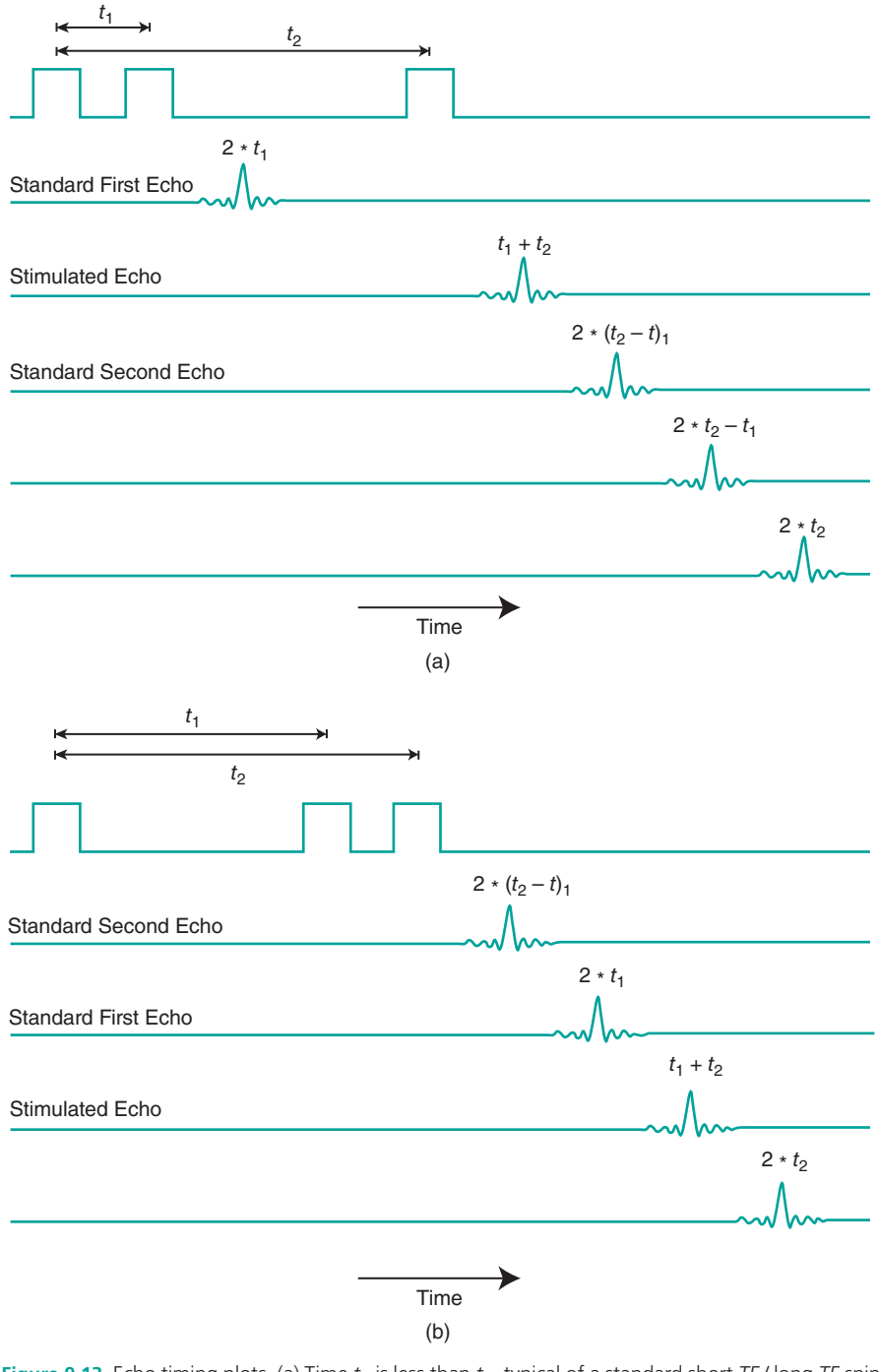

Figure 9.13 Echo timing plots. (a) Time t_1 is less than t_2, typical of a standard short *TE* / long *TE* spin echo pulse sequence. Five echoes are formed. Two are used in routine imaging (echoes 1 and 3). The stimulated echo occurs at time $t_1 + t_2$ (echo 2). (b) Time t_1 is greater than t_2, typical of a spin echo pulse sequence with a short *TE* and a spatial presaturation pulse. Four echoes are formed. Two are used in routine imaging (echoes 1 and 2). The stimulated echo occurs at time $t_1 + t_2$ (echo 3).

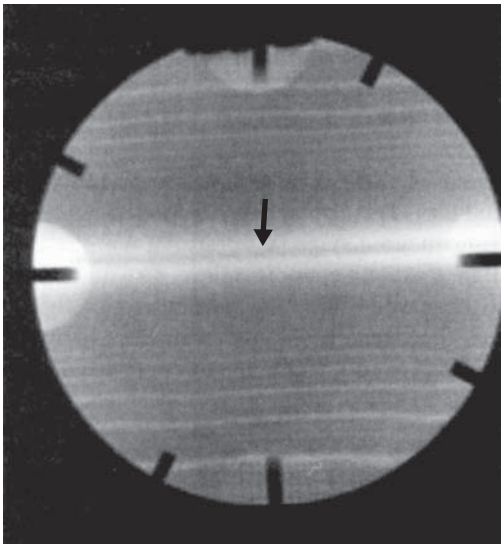

Figure 9.14 Signal contributions from undesired echoes produce banding artifacts (arrow). These echoes can be minimized through the use of coherence spoiling, either gradient-or RF-based.

echoes add in a more incoherent manner. If a sufficiently large number of phase variations is used, the net result is that the undesired signals average to zero. RF spoiling does not require additional time during the slice loop, but does require sophisticated phase modulation of the transmitter (Figure 9.15).

9.2.6 Magnetic susceptibility difference artifact

A third artifact whose appearance is sensitive to the measurement sequence is caused by differences in magnetic susceptibility χ between adjacent regions of tissue. As mentioned in Chapter 1, the magnetic susceptibility is a measure of the spin polarization induced by the external magnetic field. The degree of polarization depends on the electronic and atomic structure of the sample. Tissues such as cortical bone or air-filled organs such as lungs or bowel contain little polarizable material and have very small values for χ. Soft tissue has a greater degree of polarization and larger χ and metallic objects have an even larger χ than soft tissue. At the interface between soft tissues and the area of different susceptibility, a significant change in the local magnetic field is present over a short distance, causing an enhanced dephasing of the protons located there (see Chapter 3). As *TE* increases, there is more time for proton dephasing to occur, which results in signal loss. This dephasing is reversed by the 180° refocusing pulse in spin echo imaging since it is constant with time, but contributes to the contrast in gradient echo imaging (Figure 9.16). Magnetic susceptibility dephasing is also observed following administration of a paramagnetic contrast agent as the agent accumulates in the kidney and bladder. A significant signal loss can occur as the agent concentration in these organs increases (Figure 9.17).

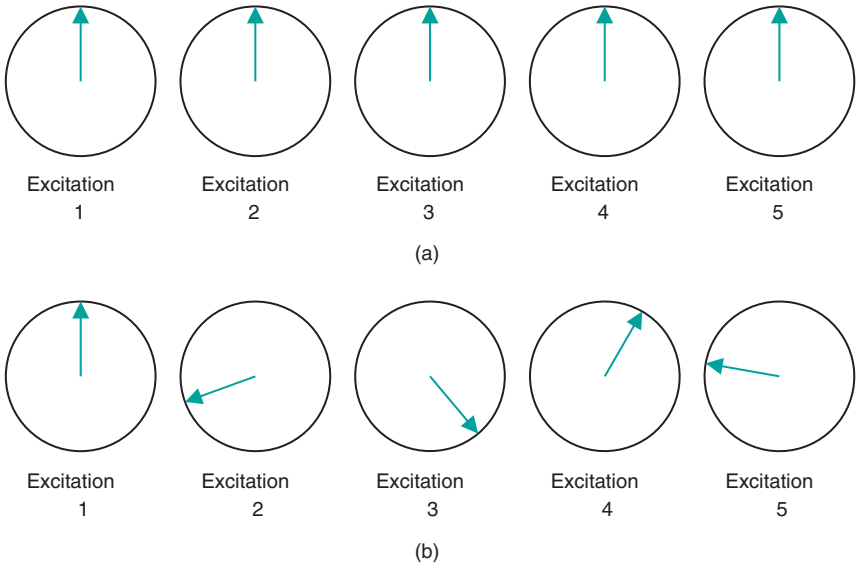

Figure 9.15 RF spoiling. (a) No spoiling. The phase of the RF excitation pulse in a rotating frame is the same for all RF pulses. The net magnetization will be rotated along the same axis following each RF excitation pulse. (b) RF spoiling. The phase of the RF excitation pulse in a rotating frame is incremented so that each RF pulse has a different phase. The net magnetization will be rotated along different axes following each RF excitation pulse.

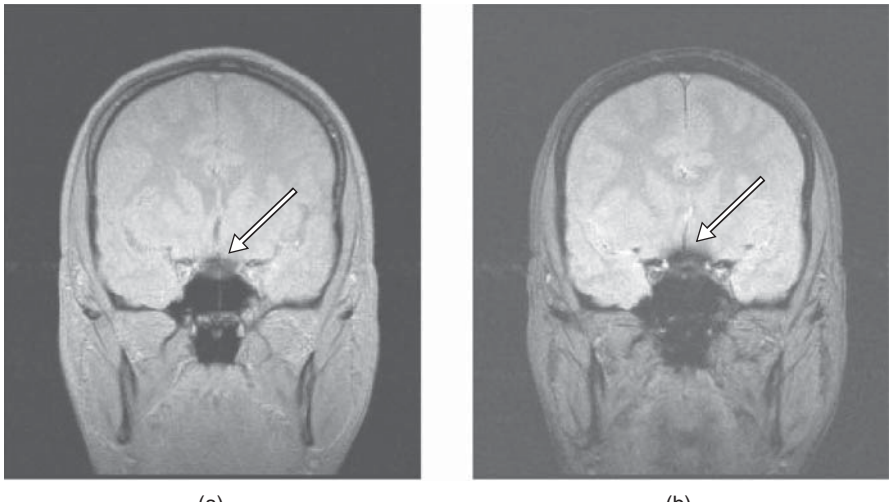

Figure 9.16 Magnetic susceptibility difference artifact. An increase in *TE* causes increased sensitivity to *T2** in gradient echo pulse sequences. Increased distortions occur in areas where there are significant differences in magnetic susceptibility, such as in the posterior fossa (arrows). Other measurement parameters: pulse sequence, two-dimensional spoiled gradient echo; *TR*, 170 ms; excitation angle, 30°; acquisition matrix, N_{PE}, 224 and N_{RO}, 256; FOV, 201 mm PE × 230 mm RO; N_{SA}, 1. (a) *TE*, 4 ms; (b) *TE*, 15 ms.

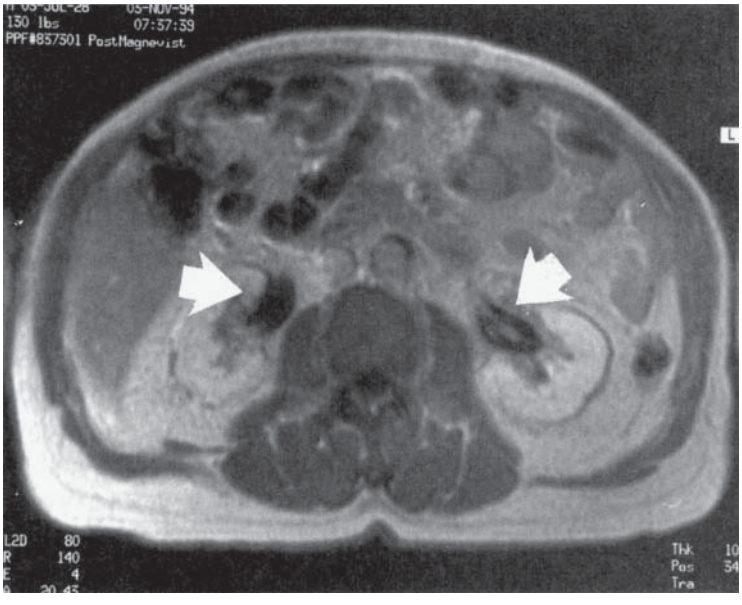

Figure 9.17 Magnetic susceptibility difference artifact. As paramagnetic contrast agents accumulate in the kidneys, the local magnetic field is distorted, causing enhanced dephasing to the protons in the vicinity and produces signal voids (arrows). Measurement parameters are: pulse sequence, two-dimensional spoiled gradient echo; *TR*, 140 ms; *TE*, 4 ms; acquisition matrix, N_{PE}, 128 and N_{RO}, 256 with twofold oversampling; FOV, 263 mm PE × 350 mm RO; N_{SA},1.

9.2.7 Radial artifact

For radial scanning (see Figure 5.18), an artifact can result if there is an insufficient number of planes sampled. This artifact is sometimes referred to as a "star" or streaking artifact and has a similar artifact found in CT scanning. An inadequate number of planes causes a breakdown in the interpolation process necessary to create the correct *k* space. The result is a streaking in the reconstructed image (Figure 9.18).

9.3 External artifacts

External artifacts are generated from sources other than patient tissue. Their appearance in the final images depends on the nature of the source and the measurement conditions. The sources may be classified into two general categories: those originating from a malfunctioning or miscalibration of the MRI hardware and those that are not. Excluded from this group are hardware problems that cause complete failure of data collection or image reconstruction. Manufacturers exert great effort to ensure that the acquired images faithfully represent the MR signals from the defined area of interest. The artifacts described here are not specific to any particular manufacturer, but can occur on any MR system.

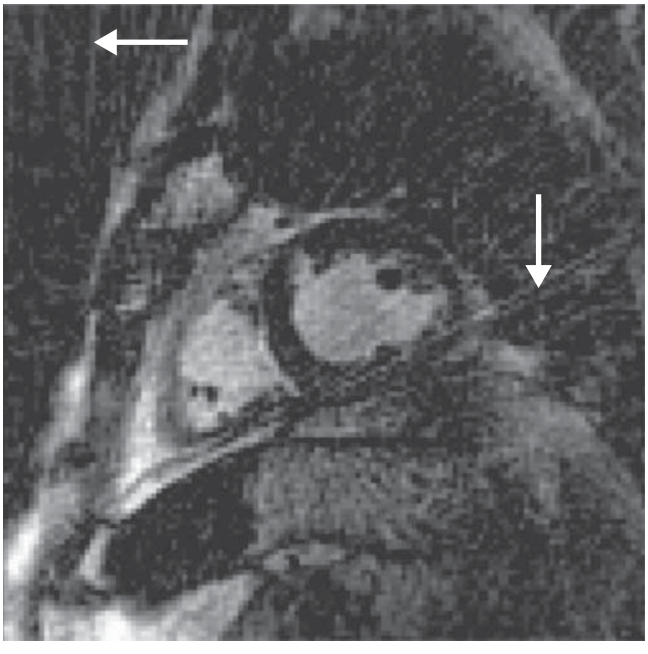

Figure 9.18 Radial artifact. Insufficient number of sample planes in a radial scan produces a scatter or "star" artifact. The primary scatter lines are indicated by the white arrows.

9.3.1 Magnetic field distortions

One of the most common system-related problems is produced by static distortions of the main magnetic field. These distortions may be due to causes related to the magnet environment or to the patient. They can cause contrast variations within the image, particularly when fat saturation is used. External causes may be transient in nature or permanent. Transient causes are typically due to unattached metal inside or near the magnet bore. These may be items such as metal clips or hooks on clothing, or staples or other removable objects. Also, items such as wheelchairs or gurneys may have metal components that alter the magnetic environment and thereby distort the magnet homogeneity. These sources can easily be eliminated by removing the metal from the vicinity of the bore. Permanent distortions to the magnetic field can be caused by metal structures surrounding the magnet (e.g., walls, cabinets) or due to manufacturing imperfections within the magnet itself. During system installation, manufacturers perform a field optimization procedure known as shimming (see Chapter 14) to eliminate coarse distortions of the central magnetic field caused by the permanent structures.

Magnetic field distortions related to the patient are typically of two types. The presence of the patient inside the magnet bore will distort the magnetic field, due to a nonuniform shape and tissue susceptibility. The other source of distortion arises from metal implants. They will deform the local magnetic field homogeneity surrounding the implant, producing significant artifacts. These artifacts frequently appear as an expansive rounded signal void with peripheral areas of high signal intensity distorting the surrounding regions, termed a "blooming" artifact. The size and shape of the artifact depends on the size, shape, orientation, and nature of the metal and the pulse sequence used for the scan (Figure 9.19). Titanium or tantalum

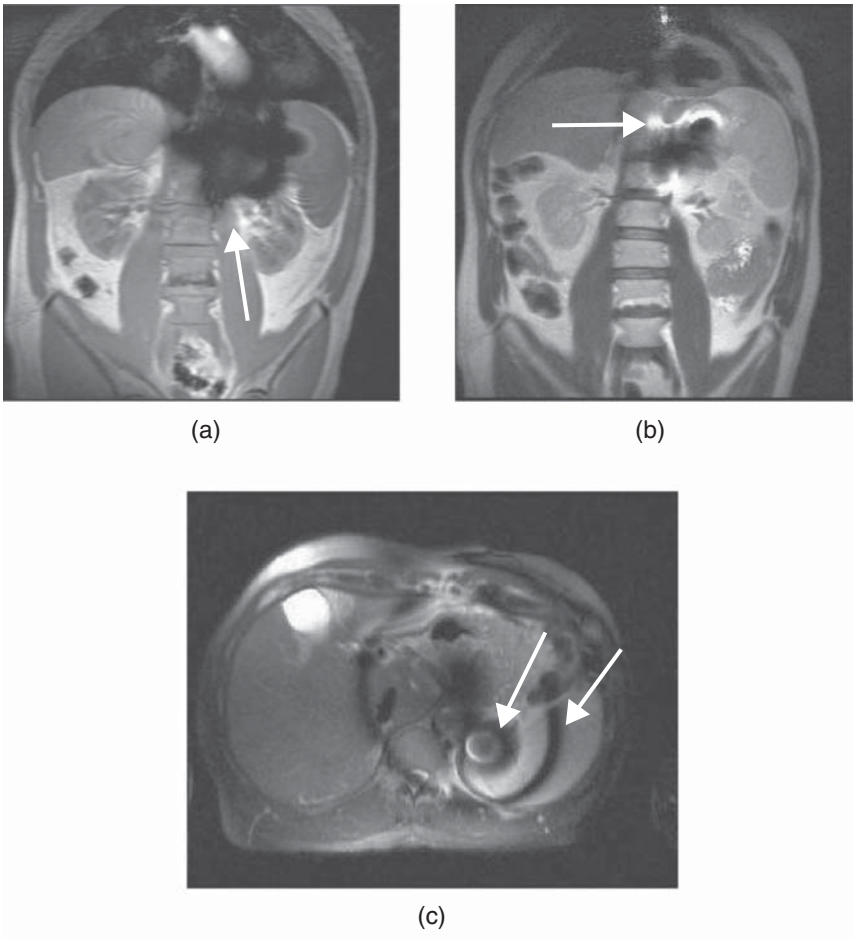

Figure 9.19 Magnetic susceptibility difference artifact. Surgical clips produce a void of signal caused due to the significant magnetic field distortion. (a) Spoiled gradient echo sequence shows significant signal distortion (arrow). (b) Single-shot echo train spin echo at the same level shows less signal loss (arrow). (c) Single-shot echo train spin echo with fat saturation shows incomplete saturation due to field distortions (arrows).

produce very localized distortions, while stainless steel can produce severe distortions that may compromise the images (Figure 9.20). All echoes are affected by the presence of the metal.

The amount of image distortion observed from static field inhomogeneities also depends on the specific measurement technique. If the field homogeneity disruption is severe, the signal loss will be enough to preclude any image whatsoever. In general, gradient echo sequences are most sensitive to field distortions. This is due to the echo signal amplitude being a function of *T2**, in which proton dephasing from magnetic field inhomogeneities is a significant factor affecting the image contrast. As in the case of magnetic susceptibility differences discussed earlier, very short *TE* values allow little time for such dephasing and result in smaller signal voids. Longer *TE* values allow more time for dephasing and can produce significant artifacts.

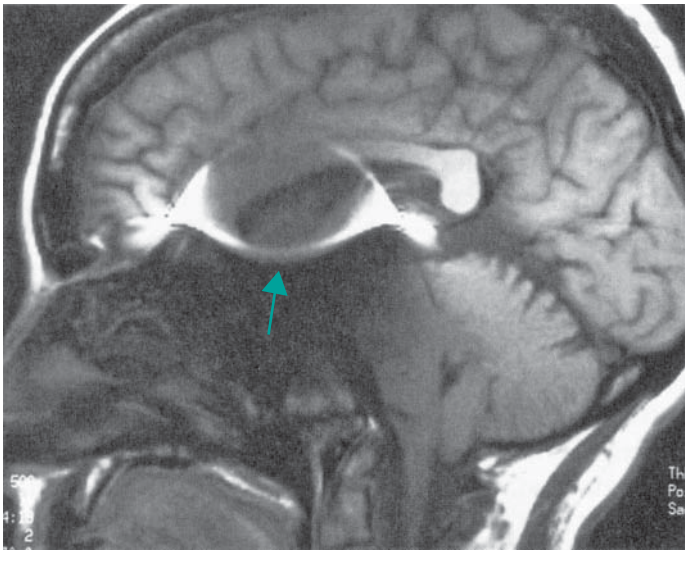

Figure 9.20 Stainless-steel aneurysm clip produces severe field distortion. Pulse sequence: spin echo.

In some instances, only spin echo sequences may produce acceptable images. Echo train spin echo techniques with short echo spacings are least sensitive to these distortions and should be used when metal is known to be in the imaging field. In addition, common metal objects within the bore, such as clothing clasps, paper clips, or staples, can cause severe image distortion.

Another instance of magnetic field distortion artifacts occurs when fat saturation is used. As mentioned in Chapter 7, fat saturation pulses are RF pulses centered at the fat resonant frequency that saturate the fat protons, leaving only the water protons to contribute to the image. If the field homogeneity is not uniform, the fat resonant frequency may vary within the image. The fat suppression pulse may not uniformly suppress the fat and may even suppress the water within the tissue. This condition results in regions of nonuniform fat suppression within the image (see Figure 8.8b) and is most commonly observed at the edges of the optimized portion of the field, as can occur in images with large FOVs or with extreme superior or inferior positions. It is advisable to try to center the anatomy within the magnet as much as possible and to perform field homogeneity correction (also called "shimming") with the patient inside the scanner prior to fat saturation.

9.3.2 Measurement hardware

Hardware-induced artifacts are those produced by malfunctioning of one or more of the scanner components during the data collection. Most MR techniques acquire multiple signals from the volume of tissue, varying only a single gradient amplitude (the phase encoding gradient) from one measurement to the next. The assumption is that any amplitude variation in the detected signal is caused by the phase encoding gradient, providing the basis for localization in that direction. One of the primary requirements of the measurement hardware for this approach to succeed is that the different subsystems act in a reliable and reproducible fashion. A lack of stability in the performance of any of the system components causes amplitude

or phase modulations or distortions in the detected signal in addition to those intrinsic to the measurement. This instability may be electronic in nature, arising from one of the electronic components of the gradient, RF transmitter or receiver, or electrical shim acting in an unreliable or inconsistent manner. It may also be mechanical in nature if the magnet, patient table, or receiver coil are not supported properly. In this case, the pulsing of the gradient coil causes motion of the patient relative to the receiver coil. The signal distortions result in smearing or ghosting artifacts in the phase encoding direction throughout the entire image field. The magnitude and nature of the instability determines the amount of smearing. In many instances, the instability artifacts are indistinguishable from motion artifacts. Manufacturers perform tests during system calibration to assess the stability of the various systems to ensure that their performance is reproducible and stable.

Proper calibration of the measurement hardware is another important contribution to high-quality MR imaging. The gradient, RF transmitter, and receiver systems are calibrated to ensure their proper performance. Improper calibration produces variable distortions, depending on which component is considered. Nonlinear gradient pulses or incorrect amplitude calibration cause incorrect spatial localization and/or image distortion. Improper RF calibration causes incorrect or nonuniform excitation power, which may or may not be noticeable in the

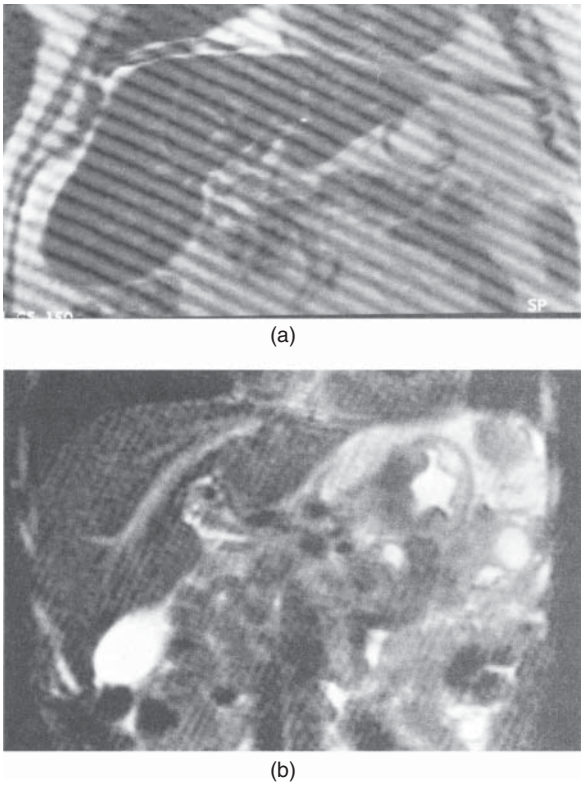

Figure 9.21 Spikes. Transient electrical discharges (spikes) during the data collection period produce a banding pattern that is superimposed across the entire imaging field. The direction and spacing of the bands depend on the timing of the discharge relative to the collection of the central phase-encoding steps.

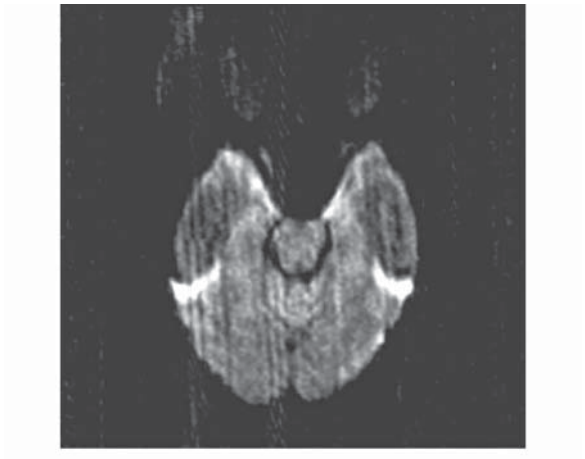

(a)

(b)

Figure 9.22 External interference: (a) artifact due to electrical source outside the scan room; (b) interference from portable patient medication unit operating in scan room during the measurement (arrows).

resulting images. The RF power deposition as measured by the specific absorption rate (SAR) will also be inaccurate. Receiver miscalibration causes incorrect amplification of the echo signal, which may result in insufficient gain so that the signal does not exceed the background noise or in excessive gain, which may cause the echo signal to exceed the digitization limits of the scanner. If parallel acquisition techniques are used, then improper balancing of the individual receiver channels can cause intensity distortions. Verification of system calibrations is normally performed during preventive maintenance of the scanner.

9.3.3 Noise

A final artifact often present in MR images is noise. Noise can have a variety of appearances, depending on the origin and nature of the source. It may appear as a film superimposed over

the normal anatomy, with or without discernible patterns, or it may have a discrete pattern or patterns. The two most common examples of coherent noise are spikes and those arising from external sources.

Spikes are noise bursts of short duration that occur randomly during the data collection. They are normally caused by static electricity discharges or arcing of electrical components, but may be generated by many different sources. Their appearance in an image depends on the severity, number, and location of the spike in relation to the signal maximum, but tend to appear as waves superimposed on the normal image data, including waves in the background (Figure 9.21). They may or may not occur in all images of the scan. Spikes are particularly problematic to isolate because they are often irreproducible, particularly if the source is static discharge.

External interference artifacts occur when there is a source of time-varying signal detected by the receiver. They appear as lines of constant frequency within the image. Their positions depend on the receiver bandwidth of the sequence and the frequency difference from the transmitter. The most common example of this is from the alternating nature (AC) of standard electrical current (60 Hz in the United States, 50 Hz in Europe and Asia) (Figure 9.22). Electrical connections for any equipment, such as external patient monitoring devices used in the scanner room, should be filtered before being allowed to penetrate the Faraday shield or the use of nonalternating (DC) current should be considered. Manufacturers should be consulted before incorporating any electrical equipment into the scan room to ensure compatibility with the MR scanner.